X-ray near-edge structure of the II-VI group ternary compounds: Experimental and theoretical studies of $Cd_xHg_{1-x}Te$ and $Cd_xZn_{1-x}Te$

A. Kisiel
Instytut Fizyki, Uniwersytet Jagielloński, Krakow, Reymonta 4, Poland

A-I. Ali Dahr and P. M. Lee
Physics Department, Lancaster University, Lancaster LA1 4YB, United Kingdom

G. Dalba and P. Fornasini
Dipartimento di Fisica, Università di Trento, I-38050 Povo (Trento), Italy

E. Burattini
Istituto Nazionale di Fisica Nucleare, Laboratori Nazionali di Frascati, I-00044 Frascati, Italy
(Received 22 January 1990)

Measurements of the x-ray-absorption edges for ternary II-VI group semiconducting compounds $Cd_xHg_{1-x}Te$ and $Cd_xZn_{1-x}Te$ have been made for the Cd and Te L edges and the K edge of Zn. These data are compared with calculations based on electron densities of states for the conduction-band states in $Cd_xHg_{1-x}Te$ and $Cd_xZn_{1-x}Te$ for $x=0.0, 0.5, 1.0$. The calculations, based on linear-muffin-tin-orbital results, cover energies up to about 17 eV above the conduction-band edge. Both the experimental data and calculated density of states are used to analyze results for the ternary compounds in terms of a virtual-crystal model based on CdTe, HgTe, and ZnTe. Using a virtual-crystal model based on the Te L_1 and L_3 x-ray edges for CdTe, HgTe, and ZnTe, predicted edges for the ternary compounds Cd-Hg-Te and Cd-Zn-Te are compared with the direct experimental data and theoretical calculations. Results obtained in these two ways are found to be in good agreement with each other.

I. INTRODUCTION

It is the aim of this paper to demonstrate that x-ray-absorption near-edge (XANES) spectra of typical zinc-blende II-VI semiconductors and also their ternary compounds can be satisfactorily described within the framework of a one-electron approximation. We leave to the future a discussion of the question of the validity of a one-electron approximation to describe the x-ray-absorption spectroscopy (XAS) of transition metals which also form ternary alloy compounds within this sequence. We have calculated conduction-band (CB) densities of states (DOS) in the energy range 0–1.3 Ry above the bottom of the CB and measured and analyzed the fine structure of the XANES energy range for the three most common binary semiconductors of the II-VI group: ZnTe, CdTe, and HgTe, which are characterized, respectively, by a wide, medium, and narrow forbidden-energy gap (2.27, 1.53, and -0.31 eV, respectively, at room temperature) and their corresponding ternary alloys Cd-Zn-Te and Cd-Hg-Te. The structure of the paper is as follows. Section II describes experimental details and the methods used in analyzing the experimental data, Sec. III presents an outline of the theoretical calculations, Sec. IV contains a discussion of the results, and Sec. V contains the conclusions.

II. EXPERIMENT AND RESULTS

A. XAS measurements

X-ray-absorption measurements have been carried out with the use of synchrotron radiation at the Adone Wiggler facility in Frascati[1] utilizing a Si(111) channel-cut crystal monochromator. The original samples were high-purity monocrystalline ZnTe, CdTe, HgTe, $Cd_{0.5}Zn_{0.5}Te$, and $Cd_{0.5}Hg_{0.5}Te$ ingots grown by the Bridgman method. To obtain thin specimens of a controlled thickness and homogeneity as required for x-ray-absorption measurements, the samples were finely powdered and deposited on polyacetate films.

XAS measurements have been made on the Te L_1 and L_3 edges for Cd-Hg-Te, Cd-Zn-Te, CdTe, HgTe, and ZnTe, Zn K edges for Cd-Zn-Te and ZnTe, and for the Cd, L_1, L_2, and L_3 edges for Cd-Hg-Te, Cd-Zn-Te, and CdTe. The energy resolution of an experimental setup of the type used in the present work is limited by the finite vertical divergence of the photon beam and a finite width of the rocking curve of the monochromating crystal. The resulting instrumental Gaussian broadening of the natural width of all measured edges has been estimated to be ~ 0.7 eV for the Te and Cd L edges and ~ 1.7 eV for the Zn K edge.

The contribution of each edge to the absorption coefficient has been isolated by extrapolating the preedge

region to a higher energy by a Victoreen-type fit and by subtracting the fitted curve from the remaining experimental spectrum.[2] Figure 1 presents the results of measurements (after subtraction of the preedge contribution) and their first derivatives for the Te, L_1 and L_3 edges in HgTe, Cd-Hg-Te, CdTe, Cd-Zn-Te, and ZnTe. Figures 2 and 3 show spectra and their derivatives for the Cd, L_1, L_2, and L_3 edges in Cd-Hg-Te, CdTe, and Cd-Zn-Te and for the Zn K edge in Cd-Zn-Te in ZnTe. Data for HgTe, CdTe, and ZnTe were taken from Ref. 3 and included for completeness.

B. Experimental data reduction

As has been shown, XANES for metals[4-9] and also for semiconductors[3,10] is described satisfactorily by the one-electron approximation; however, it is possible that in the case of transition-metal oxides such an interpretation does not work.[11] The discrepancies between theory and experiment for higher energies above the Fermi level also raise the question of the accuracy of the theoretical approaches in this energy range. According to Bloch's theorem, for an ideal infinite crystal, the electronic band structure extends throughout the energy range. In practice the calculation of the excited states above the Fermi level is limited by various factors, the immediate one being the size of the basis set used in the band-structure calculation.

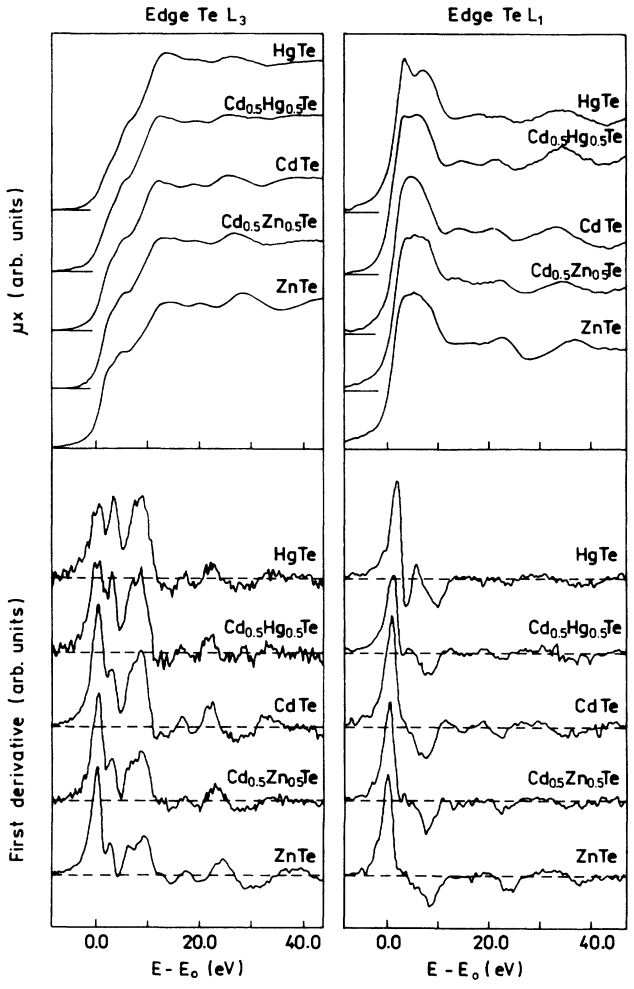

FIG. 1. Te L_3 and L_1 x-ray-absorption edges and their first derivatives for HgTe, Cd-Hg-Te, CdTe, Zn-Cd-Te, and ZnTe.

In general, for the reasons discussed in Sec. III one is rather reluctant to attach any physical meaning to the higher bands. Müller, Jepsen, and Wilkes[4] and Müller and Wilkes[5] carried out calculations for Pd up to 200 eV, but in most other calculations[3,6,7-11] the upper limit lies between 5 and 30 eV. Hence, because of the limited applicability of the one-electron approximation mentioned above and also because of the lack of a well-verified many-body theory, the explicit comparison of the theory with experiment in a whole XANES energy range is possible now only in very few cases [for instance, for Pd (Refs. 4 and 5)].

Considering the above difficulties we compared the experimental and theoretical data using the procedure of experimental data reduction proposed first by Parratt[12] for gaseous Ar and recently modified and applied to semiconductors.[3] Parratt suggested a cutoff in the upper part of the experimental spectrum and a replacement at higher energies by an arctangent curve that, according to Richtmeyer, Barnas, and Ramberg,[13] corresponds to the shape of the x-ray-absorption edge due to free electrons. It has been shown[13] that this arctangent dependence describes very well the shape of the experimental absorption L edges in Au. Thereafter we express the total absorption coefficient μ_{tot} as

$$\mu_{\text{tot}}(E;\varepsilon)=\mu_{\text{BS}}(E;\varepsilon)+\mu_{\text{FE}}(E;\varepsilon)+\mu_{\text{OS}} , \tag{1}$$

where μ_{BS} is the contribution to the total absorption from all transitions from the initial core state (assumed to possess a Lorentzian shape) to the empty CB DOS up to the energy limit ε that is arbitrarily defined by the theoretically calculated DOS; μ_{FE} is the contribution due to the transitions from the same core state to the (hypothetical) continuum of the unoccupied free-electron-like states that extend above the limit ε, and μ_{OS} is due to transitions from other core states. The last contribution may be neglected if every edge is analyzed independently eliminating contributions from other edges by the Victoreen procedure.[2] The choice of the energy ε will be discussed later. The formula (1) means that the absorption coefficient μ_{BS}, related to the CB DOS calculated up to the energy limit ε, is augmented by the absorption coefficient correlated with free-electron DOS above this limit. The term μ_{FE} in (1) is described by the integral[13,14]

$$\mu_{\text{FE}}(E;\varepsilon)=\int_{\varepsilon}^{\infty}\frac{B(E')dE'}{1-4[(E-E')/\Gamma]^2} , \tag{2}$$

where Γ is a natural Lorentzian half-width of the core state. Watanabe[15] has shown that $B(E)$ is a slowly decreasing monotonic function of energy. Hence, if after Richtmeyer, Barnas, and Ramberg,[13] we put $B(E)=\text{const}$, the integral (2) assumes a simple arctangent form

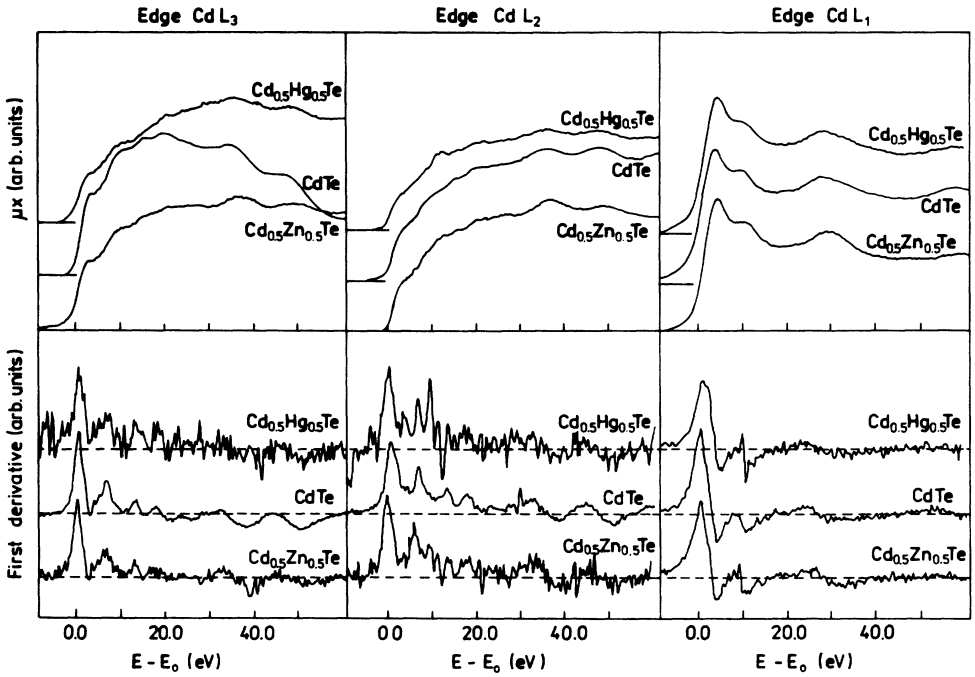

FIG. 2. Cd L_3, L_2, and L_1 edges and their first derivatives for Cd-Hg-Te, CdTe, and Cd-Zn-Te.

$$\mu_{\mathrm{FE}}=\mu_0\left[\frac{1}{2}+\frac{1}{\pi}\tan^{-1}\left[\frac{2(E-\varepsilon)}{\Gamma}\right]\right]. \tag{3}$$

Therefore, the contribution to the absorption coefficient of the band structure up to the energy limit ε can be written as

$$\mu_{\mathrm{BS}}(E;\varepsilon)=\mu_{\mathrm{tot}}(E) -\mu_0\left[\frac{1}{2}+\frac{1}{\pi}\tan^{-1}\left[\frac{2(E-\varepsilon)}{\Gamma}\right]\right]. \tag{4}$$

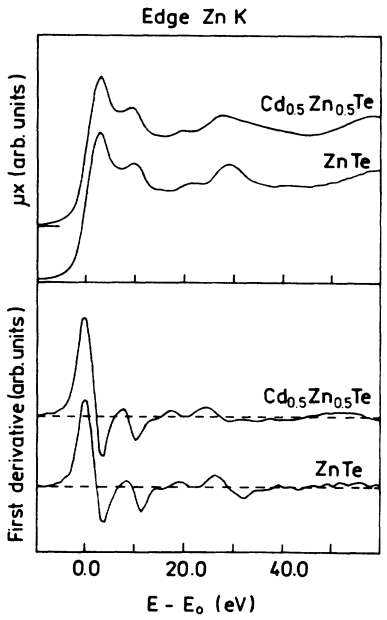

FIG. 3. Zn K edge and its first derivative for Cd-Zn-Te and ZnTe.

This expression allows for a direct comparison of the reduced experimental data with theoretical CB DOS evaluated from band-structure or other calculations and convoluted with the Lorentz function describing the initial state and the Gaussian resulting from the experimental broadening. In the formula (4) three parameter are necessary: the energy cutoff ε defined earlier, the distance μ_0 of the two asymptotes defined by the arctangent curve, the Γ parameter which is the sum of the half-widths of the Lorentzian initial state Γ_0, and the experimental broadening Γ_G and the broadening $\delta\Gamma_x$ caused by the decrease of the lifetime of the excited states in the conduction band with increasing electron energy. The last broadening estimated by Müller, Jepsen, and Wilkis[4] and Müller and Wilkis[5] can be used to evaluate the total half-width at the cutoff energy ε. The correction estimated by Refs. 4 and 5 for low energies is not very large and might be neglected.[3] We have used it, however, in all the theoretical convolution calculations; consistently it is included in our experimental data reduction procedure.

In the procedure of the experimental data reduction we have used for HgTe, CdTe, Cd-Hg-Te, and Cd-Zn-Te $\varepsilon=17$ eV and for ZnTe $\varepsilon=15$ eV (i.e., about 15 or 17 eV above the conduction-band minimum). This choice of the cutoff energy was motivated by the decreasing accuracy of the band-structure calculations as discussed in Sec. III. The value of Γ_ε used in the reduction of the experimental data has been estimated using the approximate formula

$$\Gamma_\varepsilon\simeq\Gamma_0+\tfrac{1}{2}\Gamma_G+\delta\Gamma_x\ , \tag{5}$$

in which $\Gamma_0+\frac{1}{2}\Gamma_G$ is a compromise between the two components contributing to the line shape: the Lorentzian (natural width) and the Gaussian (instrumental width)

TABLE I. Values in eV of Γ_0, Γ_G, and Γ_x used in the reduction of the experimental data.

Edge	Γ_0	Γ_G	$\Gamma_x(E=10$ eV)	Γ_x ($E=15$ eV)
Zn K	1.40	1.7±0.2	1.15	2.45
CD L_1	3.00	0.6±0.1	1.15	2.45
Cd L_2	2.15	0.6±0.1	1.15	2.45
Cd L_3	2.10	0.6±0.1	1.15	2.45
Te L_1	2.50	0.6±0.1	2.10	3.50
Te L_2	2.30	0.6±0.1	2.10	3.50
Te L_3	2.30	0.6±0.1	2.10	3.50

ones.[14] The values of Γ_0 used in the data reduction procedure are collected in Table I. They were taken from the book by Sevier[14] and also from Refs. 3,16, and 17. These values are significantly lower than those reported by Krause and Oliver.[18] They agree, however, much better with values of Γ_0 obtained from fitting experimental results with Eq. (3) for $\varepsilon=0$.[3]

The procedure for experimental data reduction presented above has two important practical features: it provides a direct comparison of the experimental data

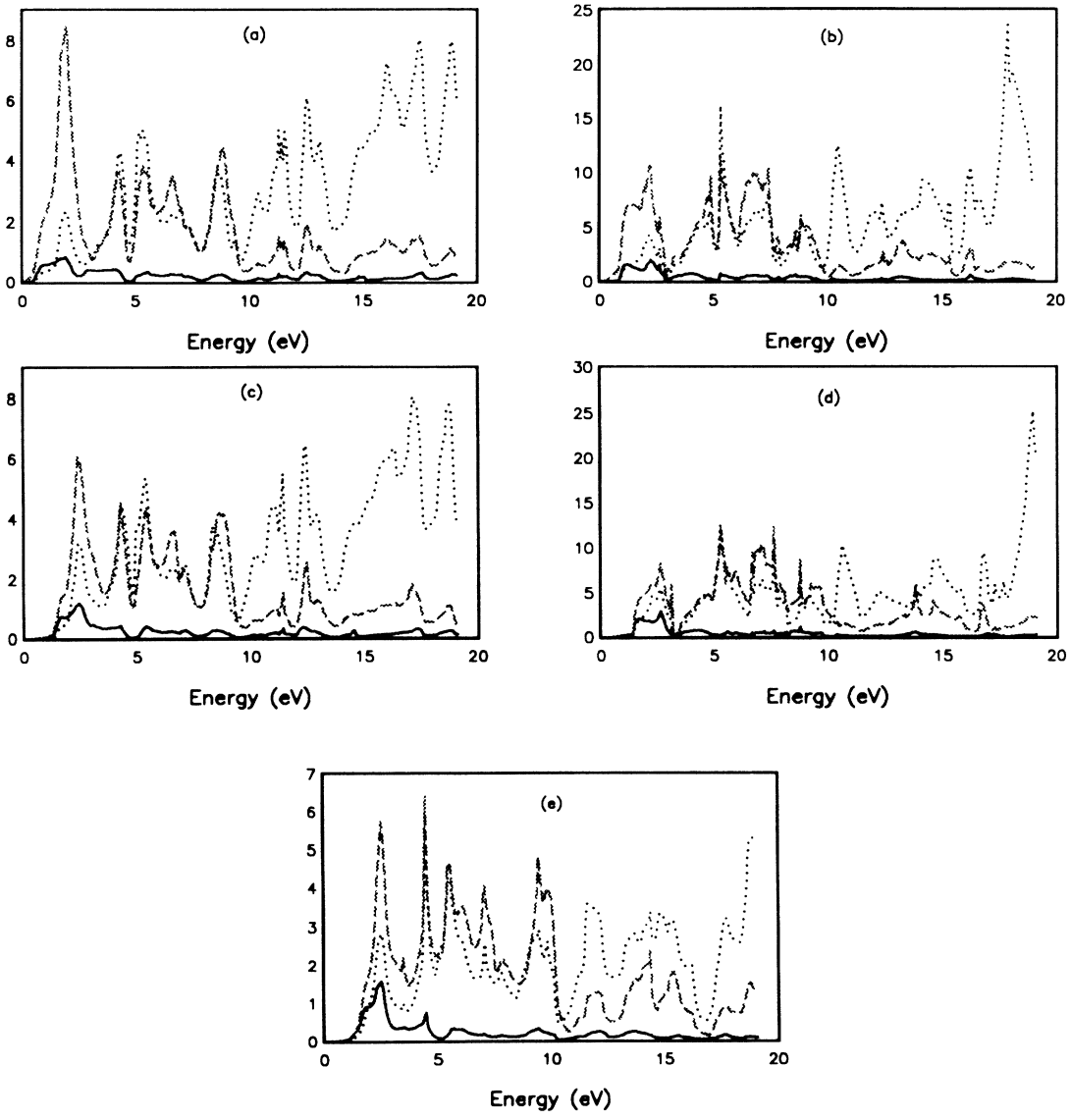

FIG. 4. Te s (solid line), p (dashed line), and d (dotted line) projected DOS for conduction-band states for HgTe (a), Hg-Cd-Te, (b), CdTe (c), Cd-Zn-Te (d), and ZnTe (e).

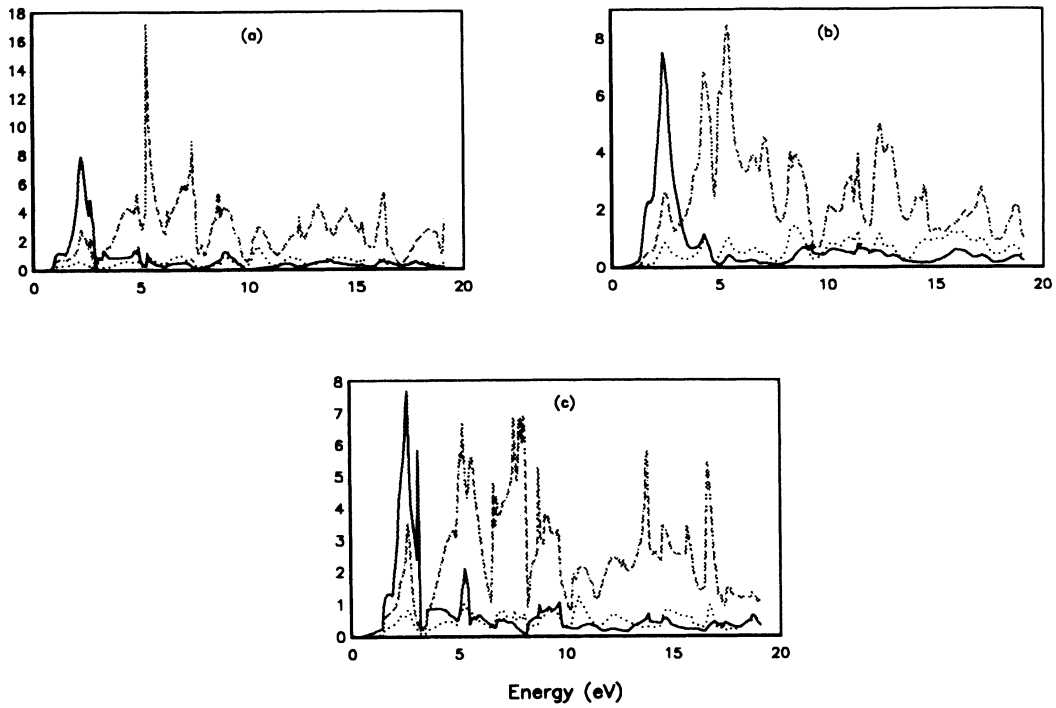

FIG. 5. Cd s (solid line), p (dashed line), and d (dotted line) projected for conduction-band states for Hg-Cd-Te (a), CdTe (b), and Cd-Zn-Te (c).

with available theoretical results whatever the range of energy might be, and it allows for a better identification of any fine structure at or near the absorption edge by scanning the experimental curve with different values of the parameter ε. It was, however, not necessary to use this facility in the present paper since there is overall good agreement between the experimental and theoretical results.

III. THEORETICAL RESULTS

Band structures and densities of states have been calculated using the linear-muffin-tin-orbital (LMTO) method[19] for the parent II-VI compounds CdTe, HgTe, and ZnTe, and for the ternary compounds $Cd_{0.5}Hg_{0.5}Te$ and $Cd_{0.5}Zn_{0.5}Te$. The structures of the parent compounds are the usual zinc-blende type, with the two atoms in the cell at positions (0,0,0) and $(\frac{1}{4},\frac{1}{4},\frac{1}{4})$ and, because of the open nature of this structure, empty spheres at $(\frac{1}{2},\frac{1}{2},\frac{1}{2})$ and $(\frac{3}{4},\frac{3}{4},\frac{3}{4})$. For the 50% ternary materials a tetragonal structure is used with four atoms plus four empty spheres in the unit cell, with units such as those above based on sites at (0,0,0) and $(0,\frac{1}{2},\frac{1}{2})$ in the cubic cell. Lattice parameters used were based on estimates calculated from the parent compounds.[20,21] These are expected to be reasonably accurate and errors arising from these estimates are likely to be small in comparison with the spread of data for peaks in the absorption coefficients. Exchange and correlation terms were included in the Hamiltonian using the von Barth–Hedin formulation.[22] This approach is known to give results for states in the conduction band which produce an energy gap that is too small by about 50%. It is interesting to note that in general the agreement between calculated and experimental

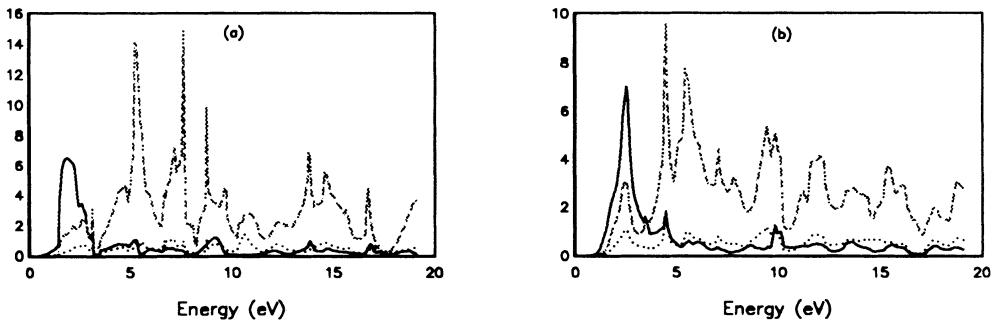

FIG. 6. Zn s (solid line), p (dashed line), and d (dotted line) projected DOS for Cd-Zn-Te (a) and ZnTe (b).

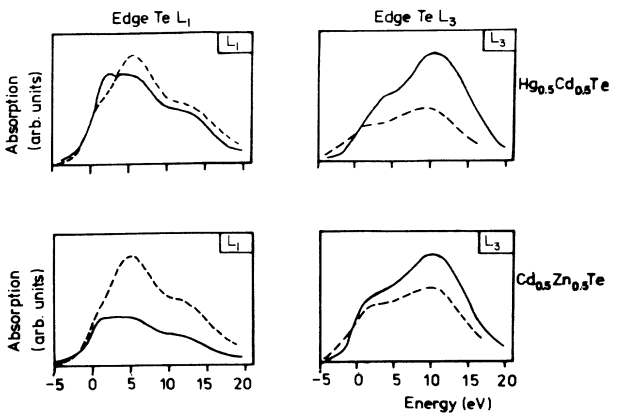

FIG. 7. Comparison of the experimental (solid line) and theoretical (dashed line) Te L_1 and L_3 edges for Hg-Cd-Te and Cd-Zn-Te.

x-ray-absorption coefficients indicates that this reduction can be considered as a shift in conduction-band levels which seems to be maintained at a constant value up to about 17 eV above the conduction-band minimum.

The band-structure density of states for these materials has been used to calculate a value for the x-ray-absorption coefficient for a number of transitions. The absorption coefficient for an x-ray photon of energy $E=\hbar\omega$ absorbed in a transition from a core state $\psi_{nlj}(j=l\pm\frac{1}{2})$ and energy $E_c=E_{nlj}$ is given by[5]

$$\bar{\mu}_c(E)=\frac{4\pi^2e^2}{3\hbar c}\frac{N}{\Omega}\frac{2j+1}{2(2l+1)}(E-E_c)^2 \times\left[\frac{l}{2l-1}f_{c,l-1}(E+E_c)+\frac{l+1}{2l+3}f_{c,l+1}(E+E_c)\right], \quad (6)$$

where N is the number of atoms in the unit cell of volume Ω. The terms $f_{c,l}$ contain the projected density-of-states contributions $N_l(E)$ for angular momentum l and the dipole matrix element $r_{c,l}(E)$:

$$f_{c,l}(E)=r_{c,l}^2(E)N_l(E)\ . \quad (7)$$

In the present analysis the dipole matrix element is taken to be independent of energy. This calculated coefficient $\bar{\mu}_c(E)$ is then corrected for lifetime effects by convoluting with a function $\Gamma(E)$ due to the core hole width Γ_c, the conduction-band excited-state lifetimes $\Gamma_x(E)$, and finally, the results are convoluted with a factor Γ_G to take account of the finite resolution of the experimental equipment,

$$\mu_c(E)=\int_{E_f}\frac{\bar{\mu}(E')\Gamma(E')dE'}{(E-E')^2+\Gamma^2(E')/4}\ . \quad (8)$$

The band-structure density of states $N_l(E)$ is taken from the angle-resolved values in the atomic spheres around the appropriate atoms associated with the initial and final states in the transition. The calculated values of $N_l(E)$ were used for a range of energy up to 17 eV above the conduction-band minimum. In this energy range arguments based on the omission of higher-order terms in $(E-E_v)$, where E_v are the pivotal energy values calculated self-consistently which are implicit in the application of the LMTO method, suggest that enough accuracy is available in the values of the density of states although the errors will increase at the higher energies in the range. The more general problem of the accuracy of the local form of the exchange and correlation potential used in describing excited states in the system is considered only in the sense that qualitative features in our comparison with the experimental data are well represented by the calculated results as was found in previous work.[3]

Calculated values of projected s, p, and d DOS for Te, Cd, and Zn are shown in Figs. 4, 5, and 6, respectively. Calculated values and reduced experimental data for the absorption coefficients are compared in Fig. 7 for Te L_1 and L_3 edges, in Fig. 8 for Cd L_1, L_2, and L_3 edges and in Fig. 9 for Zn K edges. We have used derivatives of the data shown in these graphs (Figs. 7–9) to determine an energy value to match the data. In the case of the measured values, data for the derivatives were smoothed to remove experimental scatter, and for both experiment and theory the first maximum in the derivatives is identified. The leading peaks in the derivative curves were then matched up on the energy scale and at this point of energy the calculated and measured curves for the absorption were made equal as a measure of normalization to compare the results. As near as possible this then ensures that the required coincidence at the edge is obtained.

IV. DISCUSSION

Looking at Figs. 7–9 it is seen that the agreement between the experimental and theoretical x-ray-absorption edges for ternary Cd-Hg-Te and Cd-Zn-Te is in general quite good. The agreement also confirms that for ternary semiconducting II-VI group compounds a one-particle interpretation can be applied. However, a more detailed comparison of the results with a previous analysis[3] for binary compounds ZnTe, CdTe, and HgTe shows up some discrepancies. In particular, when we look at the results for transitions from s-like core states to p-like projected components (edges K and L_1) such discrepancies reflect the fact that the p-like conduction-band states are modified nonlinearly during alloying with either Zn or Hg, whereas the s and d states behave much more linearly. Also the L edges of Cd are better reproduced by the theory than the L edges of Te, and this fact may also be related to the reasons previously given.

A virtual-crystal model has also been used to interpret the results. A rigorous justification of such a model is difficult and it is known[23,24] that such an approach fails to explain features in the ultraviolet photoemission spectroscopy (UPS) and x-ray photoemission spectroscopy (XPS) spectra relating to states that have a tendency to be more localized around a given atomic site. Thus states that are low lying in energy in the valence band (s, p, and, in particular, d bands) in these materials would probably

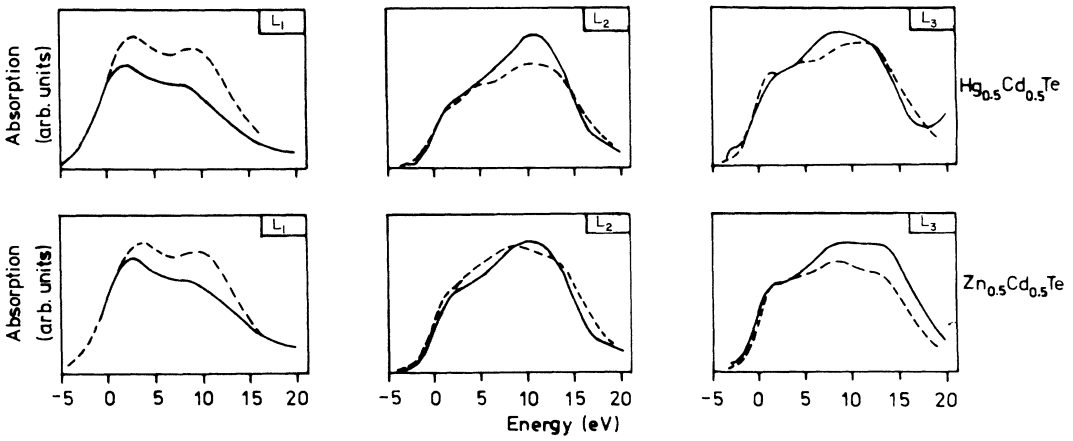

FIG. 8. Comparison of the experimental (solid line) and theoretical (dashed line) Cd L_1, L_2, and L_3 edges for Hg-Cd-Te and Cd-Zn-Te.

be better dealt with by single-site theories such as the coherent-potential approximation. In fact, the band calculations for the ternary compounds show a complex structure of valence d bands with the distinct features of the two cations present. The results indicate that such band states are quite localized around the atomic sites of Cd, Zn, or Hg and that little hybridization occurs between them and the valence s and p bands. However, states in the conduction band do not show such localization and we believe we are justified in using a virtual-crystal model in these circumstances.

To this end Te L edges for the compounds Cd-Hg-Te and Cd-Zn-Te are compared with predictions obtained by applying the virtual-crystal model using the experimental Te L x-ray edges for the basic compounds. For example, values for $Cd_{0.5}Hg_{0.5}Te$ have been obtained from

$$0.5CdTe+0.5HgTe=Cd_{0.5}Hg_{0.5}Te\ .$$

Results from this model are compared with direct measurements in Figs. 10 and 11. The analysis using the model is limited to energies up to about 20 eV in the case of $s\rightarrow p$ transitions when agreement becomes less good [see Fig. 10(b)]. However, for $p\rightarrow sd$ transitions agreement is obtained to much higher energies [see Fig. 10(e)]. This agreement is also seen in a direct comparison of the experimental and theoretical data for the Te L_1 and L_3 edges, because also in that case there is a problem of the nonlinear contribution of both the cation wave functions and their corresponding potentials. The same features exist for Cd-Zn-Te (Fig. 11). An interesting feature, particularly in the case of Cd-Zn-Te (Fig. 11), is the different extended x-ray-absorption fine-structure (EXAFS) oscil-

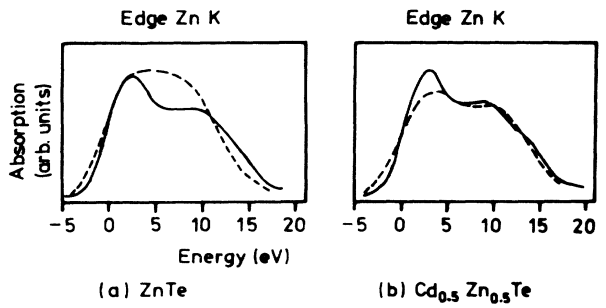

FIG. 9. Comparison of the experimental (solid line) and theoretical (dashed line) Zn K edges for ZnTe (a) and Cd-Zn-Te (b).

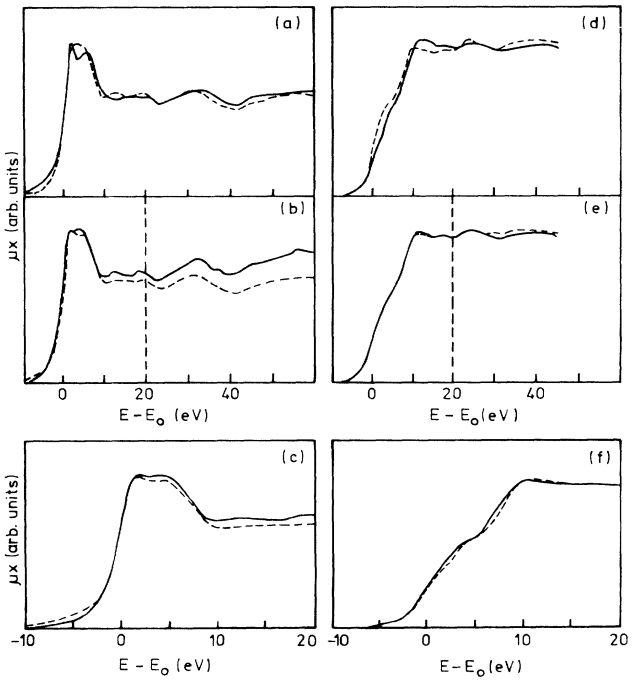

FIG. 10. Comparison of Te L_1 and L_3 edges for $Cd_{0.5}Hg_{0.5}Te$ with predictions obtained from applying the virtual-crystal model formula $0.5CdTe+0.5HgTe=Cd_{0.5}Hg_{0.5}Te$. (a) and (d) experimental edges for HgTe (solid line) and CdTe (dashed line) normalized to the inflection point of the data. (b) and (e) Experimental edges Cd-Hg-Te (solid line) and Cd-Hg-Te (dashed line) predicted from basic components. (c) and (f) The same as in (b) and (e) on an enlarged energy scale (-10, 20 eV).

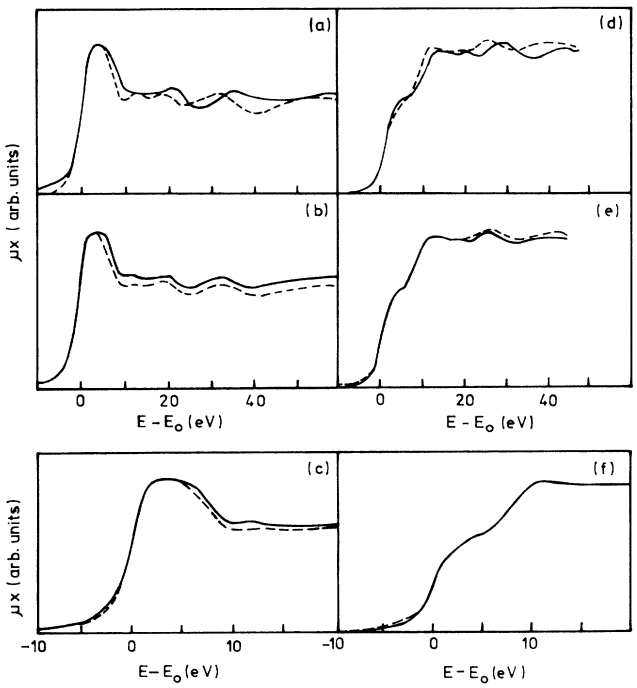

FIG. 11. Comparison of Te L_1 and L_3 edges for $Cd_{0.5}Zn_{0.5}Te$ with predictions obtained from applying the virtual-crystal model formula $0.5CdTe+0.5HgTe=Cd_{0.5}Hg_{0.5}Te$. (a) and (d) Experimental edge for ZnTe (solid line) and CdTe (dashed line) normalized to the inflection point of the data. (b) and (e) Experimental edges Cd-Zn-Te (solid line) and Cd-Zn-Te* (dashed line) predicted from basic components. (c) and (f) The same as in (b) and (e) on an enlarged energy scale (-10, 20 eV).

lations (for energies higher than 15 eV) for pure CdTe and ZnTe, which still leaves good agreement with the virtual-crystal calculations, and a similar structure for the mixed compounds is produced from distinctly different components [see Figs. 11(b) and 11(e)]. The above results of the experimental data analysis obtain

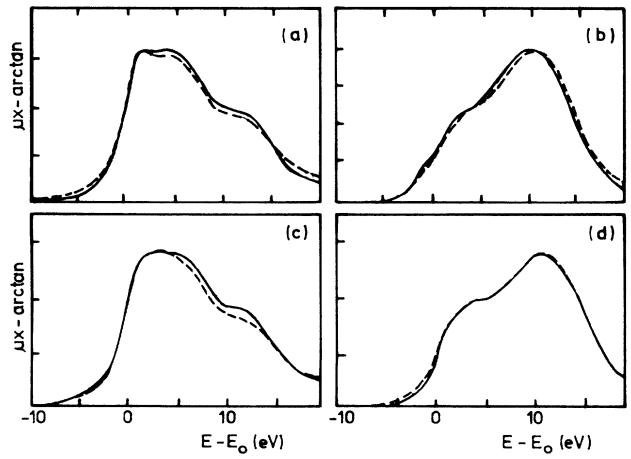

FIG. 12. Comparison of the reduced experimental absorption coefficients, as defined by Eq. (4), of Cd-Hg-Te [(a) and (b)] and Cd-Zn-Te [(c) and (d)] with virtual-crystal predictions for Te L_1 and L_3 edges. Dashed lines represent the virtual-crystal predictions.

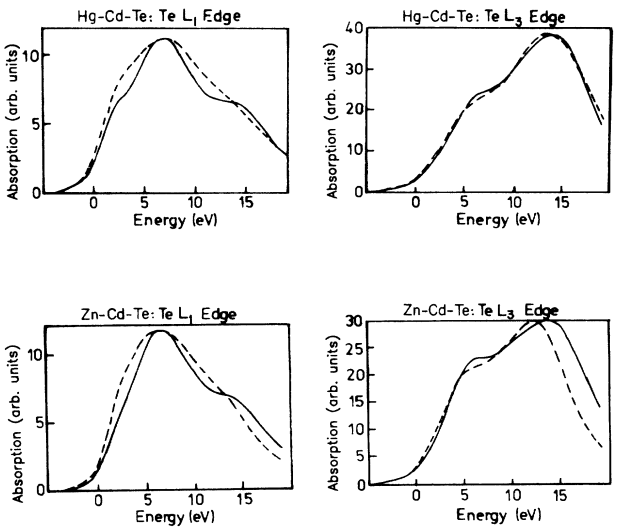

FIG. 13. Comparison of the virtual-crystal theoretical results for Te L_1 and L_3 edges in Cd-Hg-Te and Cd-Zn-Te. The solid line represents results calculated directly and the dashed line those using the virtual-crystal model and results for the binary compounds CdTe, HgTe, and ZnTe. Coefficients are constructed from CdTe and ZnTe components.

support from an application of the virtual-crystal approximation (VCA) to the theoretical absorption coefficients. Figures 12 and 13 show, in the frame of the VCA, a consistency and good agreement for both experimental and theoretical analysis, apart from the fact that the Te-projected DOS differ significantly for binaries as well as for ternary compounds (see Fig. 4). This success is mainly the result of the projected DOS averaging which occurs due to the relatively large Lorentzian half-width of the initial state and the experimental broadening.

Looking at the construction of the absorption coefficients of ternary compounds from binary com-

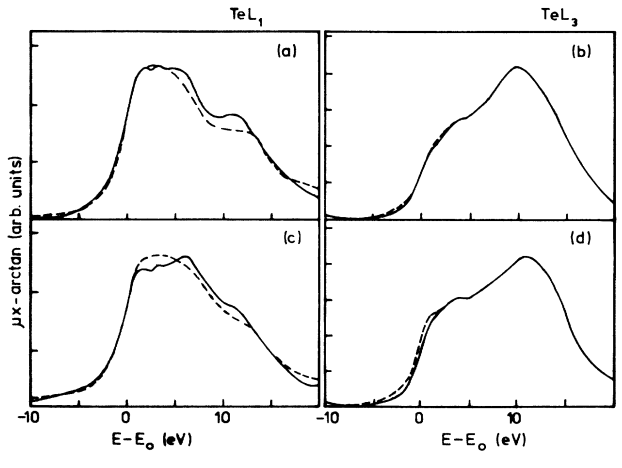

FIG. 14. Contributions of the binary materials CdTe [(a) and (b)] and ZnTe [(c) and (d)] extracted from Cd-Zn-Te (experimental data) reduced according to Eq. (4) using the virtual-crystal model formulas $Cd_{0.5}Zn_{0.5}Te-0.5ZnTe=0.5CdTe$ [(a) and (b)] and $Cd_{0.5}Zn_{0.5}Te-0.5CdTe=0.5ZnTe$ [(c) and (d)].

ponents, obviously the same VCA procedure can be applied also for extracting binary components from ternary edges using the simple formula

$$A_{1-x}B_xC-(1-x)AC=x(BC)\ .$$

An application of this formula for $Hg_{0.5}Cd_{0.5}Te$ and $Cd_{0.5}Zn_{0.5}Te$ is presented in Fig. 14.

V. CONCLUSIONS

Measurements of XAS over an energy range 0–60 eV above the x-ray edge have been made and yield detailed data for the transitions concerned in CdTe, HgTe, ZnTe, Cd-Hg-Te, and Cd-Zn-Te. These experimental results have been found to be in good agreement with conduction-band densities of states calculated by the LMTO method in the energy range 0–17 eV above the conduction-band minimum. It also confirms that the x-ray edges for ternary semiconducting II-VI compounds are described satisfactorily by a one-electron approximation. In addition a virtual-crystal model for the ternary compounds using experimental data from CdTe, HgTe, and ZnTe has predicted results for Cd-Hg-Te and Cd-Zn-Te whose agreement with the experimental and the theoretical calculations is satisfactory. For the future, it will be interesting to see if the same features and predictions are observed in the ternary alloys Cd-Mn-Te and Zn-Mn-Te.

ACKNOWLEDGMENTS

We wish to thank Professor W. Giriat and Professor A. Mycielski for supplying the samples for the studies. Also we would like to thank Dr. A. Balerna, Dr. E. Bernieri, and the technical staff at the PWA group of the Laboratori Nazionali di Frascati for their help and hospitality. One of us (A.K.) gratefully acknowledges the University of Trento, the Centro di Fisica degli Stati Aggregati ed Impianto Ionico Comitato Nazionali di Recherche Trento (CNR-ITO) Research Centre of Trento, and the National Institute of Nuclear Physics (INFN) in Frascati for financial support during the preparation of this work. This work was supported in part by the Polish Central Research Program No. CPBP 01.12.

[1]E. Burattini, E. Bernieri, A. Balerna, C. Menuccini, R. Rinzivillo, G. Dalba, and P. Fornasini, Nucl. Instrum. Methods A **246**, 125 (1986).

[2]B. K. Teo, *EXAFS: Basic Principles and Data Analysis,* SERIA (Springer, Berlin, 1986), Vol. 9.

[3]A. Kisiel, G. Dalba, P. Fornasini, M. Podgorny, J. Oleszkiewicz, F. Rocca, and E. Burattini, Phys. Rev. B **39**, 7895 (1989).

[4]J. E. Müller, O. Jepsen, and J. W. Wilkis, Solid State Commun. **42**, 365 (1982).

[5]J. E. Müller and J. W. Wilkis, Phys. Rev. B **29**, 4331 (1984).

[6]V. C. Kostroun, W. Fairchild, C. A. Kukkonen, and J. W. Wilkis, Phys. Rev. B **13**, 3268 (1976).

[7]Raju P. Gupta and A. J. Freeman, Phys. Rev. Lett. **36**, 1194 (1976).

[8]J. E. Müller, O. Jepsen, O. K. Andersen, and J. W. Wilkis, Phys. Rev. Lett. **40**, 720 (1978).

[9]T. K. Sham, Phys. Rev. B **29**, 1888 (1984).

[10]C. Sagiura and S. Muramatsu, Phys. Status Solidi B **129**, K157 (1985).

[11]B. Poumellec, J. E. Maruco, and B. Tonzelin, Phys. Rev. B **35**, 2284 (1987).

[12]L. G. Parratt, Phys. Rev. **56**, 295 (1939).

[13]E. K. Richtmeyer, S.W. Barnas, and E. Ramberg, Phys. Rev. **46**, 843 (1934).

[14]K. D. Sevier, *Low Energy Electron Spectroscopy* (Wiley Interscience, New York, 1972).

[15]T. Watanabe, Phys. Rev. **137**, A1380 (1965).

[16]E. Noreland, Ark. Phys. **26** 341 (1964).

[17]M. A. Blokhin, *The Physics of X-Rays,* 2nd ed. (Mir, Moscow, 1957).

[18]M. O. Krause and J. H. Olivier, J. Phys. Chem. Ref. Data **8**, 329 (1979).

[19]O. K. Andersen, Solid State Commun. **13**, 133 (1973).

[20]K.C. Hass and D. Vanderbilt, *Proceedings of the 18th International Conference on the Physics of Semiconductors, Stockholm, 1986* (World Scientific, Singapore, 1987) pp. 1181–1184.

[21]N. Motta, A. Balzarotti, P. Letardi, A. Kisiel, M. T. Czyżyk, M. Zimnal-Starnawska, and M. Podgòrny, Solid State Commun. **53**, 509 (1985).

[22]U. von Barth and L. J. Hedin, J. Phys. C **5**, 1620 (1972).

[23]J. A. Silbermann *et al.*, J. Vac. Sci. Technol. **21**, 142 (1982).

[24]K. C. Haas and R. J. Baird, Phys. Rev. B **38**, 3591 (1988).